A supervised learning model to capture ablation of heat shields

Vijay B. Mohan Ramu[1] and Savio J. Poovathingal[1]

1Department of Mechanical and Aerospace Engineering, University of Kentucky, Lexington, KY, USA 40506

Keywords: Ablation, heat shields, recession rate, direct simulation Monte Carlo (DSMC), supervised learning, support vector regression (SVR).

Abstract Heat shields regulate the temperature of space capsules when subjected to an environment with high aerodynamic heating. Carbon phenolic composites exhibit high heat dissipation rates with a minimum weight penalty, which serves as an attractive solution to regulate the temperature of space capsules. The performance of carbon phenolic composites as heat shields is dependent on the thermochemical processes experienced by the space capsules during entry. The underlying thermochemical phenomena are multi-scale in nature, with changes in the fibers (mesoscale) of carbon composites affecting the macroscale ablation of the carbon composite surface. State-of-the-art macroscale solvers rely on empirical formulations for closure as they cannot inherently resolve the effects of mesoscale changes on the macroscale phenomena. To address the closure problem, we propose a supervised learning model inspired by conventional neural networks developed for spatio-temporal systems. A custom surface function captures the evolution of the carbon microstructure, serving as an encoder/decoder in the model. Support Vector Regression (SVR) forms the hidden layer by operating on the reduced dimensional space of the encoder/decoder framework. The newly trained model is capable of predicting the recession rate instantaneously and provides a pathway to incorporate the effect of material microstructure into macroscale solvers.

1 Introduction

Carbon composites act as insulators for space capsules, aircrafts, and nuclear fusion reactors [1, 2, 3]. Depending on the type of matrix employed, carbon composites are broadly classified into carbon-carbon and carbon-phenolic composites. A carbon-carbon composite consists of carbon matrix in contrast to a carbon phenolic composite, which contains a phenolic matrix [4]. Irrespective of the matrix employed, carbon composites react with dissociated air at temperatures above 800 K [5]. The reactions result in continuous removal of material from the surface resulting in ablation of the surface. Surface recession is a macroscale effect that is directly influenced by mesoscale changes of carbon microstructures. It is intractable for macroscale solvers to account for mesoscale changes of the material during ablation without a closure model because of the disparate length scales between the fibers ($O(100\mu\text{m})$) and macroscale system ($O(\text{m})$) [6]. A mathematical model capable of capturing the physical changes in carbon microstructures can allow the inclusion of mesoscale effects into macroscale recession.

In the current work, we limit ourselves to carbon phenolic composites used as a protective layer for space capsules during re-entry [7]. The carbon phenolic composites generally consist of a porous carbon fiber network impregnated with phenolic resin. The phenolic resin decomposes at 500 K and ejects into the outer environment as pyrolysis gases, exposing the carbon microstructure network (char layer) to the high-temperature gas. The high porosity of the carbon microstructure allows the high-temperature gas to diffuse into the exposed char layer and facilitates material removal through both surface and volume ablation. The removal of material increases the porosity of the exposed microstructure, which enhances the diffusion of the high-temperature gas. This self-sustaining process continues until the entire heat shield is consumed or the mission comes to an end. Figure 1 represents the char layer of a carbon phenolic composite exposed to hot dissociated gas.

Detailed mesoscale simulation of carbon microstructures which represents the exposed char layer (Figure 1) during reentry have been performed using stochastic particle-based approaches like Monte

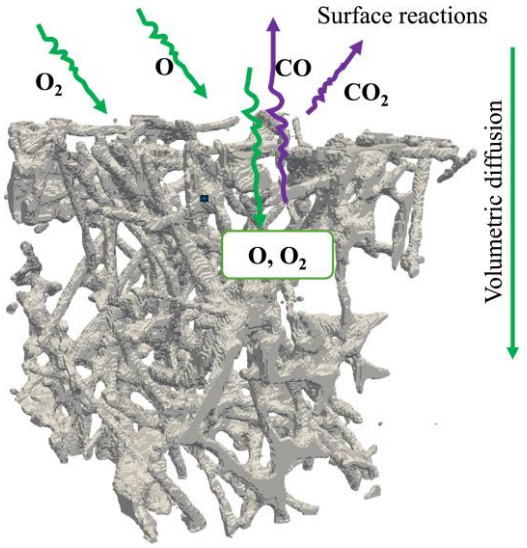

Figure 1: Char layer exposed to hot dissociated gas.

Carlo direct simulation (DSMC) [8]. These mesoscale simulations have provided valuable insights into the type of degradation of carbon fibers depending on the reaction probabilities of carbon fibers with hot dissociated gas [4].

A pictorial representation of two different scenarios for ablating microstructures is shown in Figure 2 [9]. In Figure 2(a), the needle-like degradation of carbon fibers primarily takes place on the fibers exposed to the flow, resulting in the carbon microstructure receding layer by layer. Previous works on this topic have observed similar degradation for high surface reaction probabilities (α) where α is the probability that a gaseous atom or molecule reacts with solid carbon to form gaseous carbonaceous products [4]. However, when the reaction probabilities of gas-surface interactions are very low, oxygen atoms diffuse evenly throughout the microstrucutre without spontaneously forming oxidized products at the carbon fibers exposed to the flow [4]. This type of degradation results in the thinning (Figure 2(b)) of all carbon fibers instead of needle-like degradation (Figure 2(a)). The changes in the type of degradation observed with varying microscopic reaction probabilities directly affect surface recession rate. State-of-the-art macroscale solvers employ empirical formulations obtained from physical experiments on vitreous carbon surfaces [10]. As a result, macroscale solvers overlook mesoscale parameters that influence surface recession such as defects in carbon composites, volumetric diffusion of gases, and fiber degradation. In order to bridge this gap between mesoscale and macroscale phenomena, we utilize machine learning techniques to propose an effective surface recession model that depends on the evolution of the microstructure.

Historically, Long short term memory (LSTM) [11] networks have been used as supervised learning models to solve the underlying spatio-temporal systems with varying degrees of success. LSTM in particular boasts an impressive record of its successful application to spatio-temporal non-linear dynamical systems [12, 13, 14] and microstructure evolution problems [15]. However, the application of LSTMs are only limited to predicting the future rather than learning the inherent non-linear dynamical phenomena driving the underlying problem [16]. To better suit the needs of our current application, we propose to explore a framework inspired from previous works, which are proven to perform well in capturing the physical phenomena driving the underlying spatio-temporal system [17, 18]. The training data for the custom framework consists of snapshots depicting the physical changes of the

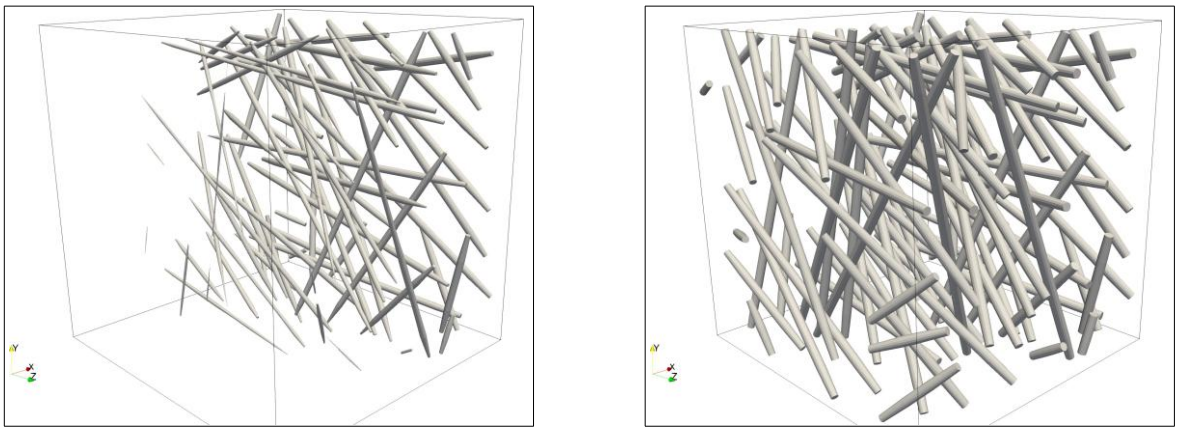

(a) (b)

Figure 2: Oxidation of a synthetic char layer with two different reaction probabilities.

microstructure that are obtained through coupled flow-material simulations [19]. A custom surface function which acted as both an encoder and decoder of the supervised learning model is used to capture the profile of the evolving microstructure. Support Vector Regression (SVR) formed the hidden layer of the model by relating the surface function parameters with input variables (porosity, time, and microscopic probabilities). The output of the SVR is then utilized by the decoder to reconstruct the profile of the microstructure. Further, the changes in the profile of the microstrcuture can be utilized to determine the recession rate. The initial proposed architecture of the supervised learning framework and the various tools used to realize the framework are explained in Sec. 2. The supervised learning model developed to predict the recession rate of a carbon phenolic composite is presented in Sec. 3.

2 Methods

2.1 Predictive model architecture and the surface function

The workflow of the developed supervised learning model is represented by Figure 3. The supervised learning model consists of a custom hidden layer (SVR) and an encoder/decoder layer to predict the evolution of the microstrucutre.

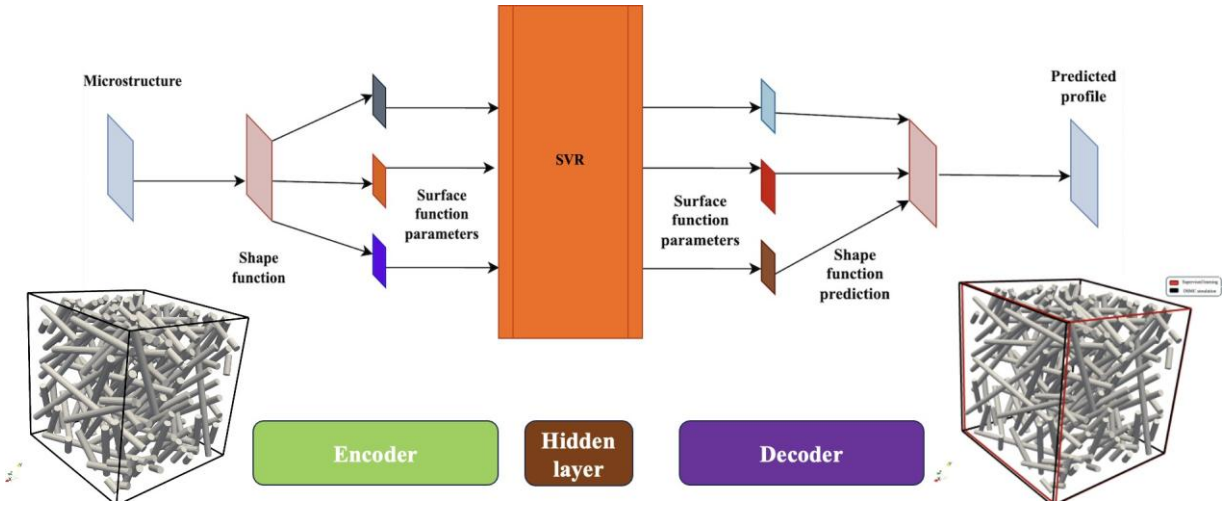

Figure 3: Flow chart of the various components present in the supervised learning model.

In our current work, a shape function capable of capturing the profile of the char layer acts as both an encoder and a decoder. The main idea behind the utilization of a shape function is to capture the necessary physical changes of a char layer subject to oxidation, with the help of an analytical function. This analytical function, also referred to as the shape function, is defined by a set of parameters that can be tracked to reconstruct the original structure of the char layer at any given instant of time. As part of preliminary work, we look at the degradation of a char layer at different time intervals (Figure 4(a) and Figure 4(b)) to infer the changes in the profile of a char layer subject to oxidation. As represented by Figure 4, the char layer is enclosed by a cuboidal profile with five constant faces (planes) and a single moving face (plane). We assume one of the constant faces as a reference plane and define the moving plane as a plane parallel to the reference plane at a distance of $h = f(t)$ from the reference plane. We particularly choose h to be in the direction of the flow (y- axis) to ensure that the newly defined parameter provides a direct measure of the recession rate of the char layer.

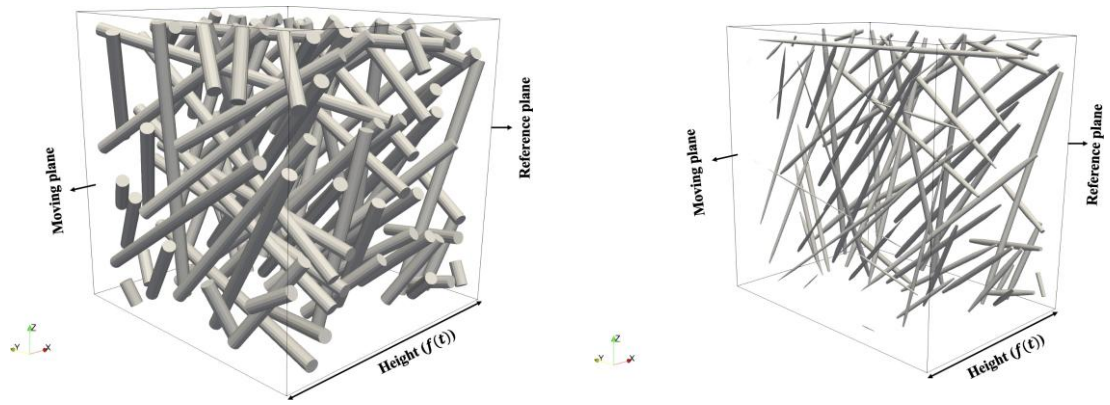

(a) (b)

Figure 4: Char layer subject to oxidation at two different intervals of time.

For the above case (Figure 4), evaluating dh/dt will provide the recession rate of the char layer. From the above observations we can define the surface function as Equation 1.

$$SF = a(x - x_o) + b(y - (y_o + h(t)) + c(z - z_o) = 0 \quad (1)$$

The case considered in this section involves different instances of the same synthetic microstructure which implies that h is a function of time alone. However, the current scope of study requires a more general form of Equation 1 where h is a function of porosity, time, and microscopic reaction probability, as given by Equation 2.

$$SF = a(x - x_o) + b(y - (y_o + h(\phi, t, \alpha)) + c(z - z_o) = 0 \quad (2)$$

Equation 2 consists of a single parameter h that defines the surface function. Effectively tracking the variation of h with input parameters (ϕ, t, α) helps in predicting the oxidation profiles of a char layer. The new parameter defined by the surface function is modeled by the hidden layer and can be separately expressed as a function of input parameters such as porosity, time and microscopic reaction probabilities. By using the surface function, we can reduce the underlying problem statement into a set of unknowns varying with input parameters (porosity, time, and microscopic reaction probabilities).

2.2 *Hidden layer and Support Vector Regression (SVR)*

Support Vector Regression (SVR) forms the hidden layer of our model which helps in finding the non-linear relationship between the new set of parameters defined by the shape function with the input parameters (porosity, time and microscopic reaction probabilities). SVR is a robust and flexible regression technique based on support vector machines (SVM), first identified by Vapnik and his colleagues in 1992 [20]. SVR is a non-parametric regression technique as it relies on kernel functions to project the data points onto a higher dimensional space. Once transformed by the kernel function, a dual minimization problem is solved on the training data in order to find the non-linear function relating the inputs to the output. A detailed mathematical formulation of the SVR problem involved in the current study can be found in the documentation of the Scikit-learn module [21]. The predictive function after implementing SVR on a set of training vectors is given by Equation 3.

$$f(x) = \Sigma_i^n(\boldsymbol{\alpha_i} - \boldsymbol{\alpha_i^*})G(\boldsymbol{x_i}, \boldsymbol{x}) + b \tag{3}$$

where $\boldsymbol{x_i}$ are the support vectors obtained from training, n is the number of support vectors, $(\boldsymbol{\alpha_i} - \boldsymbol{\alpha_i^*})$ are the dual coefficients, $\boldsymbol{x}$ is the input vector, $G(\boldsymbol{x_i}, \boldsymbol{x})$ is the kernel function, and b is the intercept. In this work, a Gaussian function is used as the kernel function (G) to approximate the random errors associated with the stochastic process. The hyper-parameters involved in the SVR formulation [21] are further fine tuned to validate the predictive model.

We conclude the current section by outlining the necessary steps required to realize the predictive model. First, we process the microstructural images recorded from the repeated material-flow simulations [19] depicting the degradation of the char layer. Next, the processed images are converted into the surface function parameter (h), where each image corresponds to a tabulated training case. The tabulated data are utilized by the hidden layer to formulate the SVR function (Equation 3) for the defined surface function parameter (h). The SVR function is capable of predicting the value of the surface function parameter depending on the user defined input variables (ϕ, t, α). Finally, the predicted surface function parameter can be used to re-construct the profile of the char layer. Further, by evaluating dh/dt, we can obtain the recession rate associated with the char layer with varying ϕ, t, and α.

3 Results

3.1 *Developed custom supervised learning framework*

The crux of the involved spatio-temporal system lies in the capability of the SVR formulation to capture the non-linear relationship between the surface function parameter with the user defined input variables (ϕ, α, and t). A robust sampling scheme must be adopted to represent the training domain. Hence, we make use of Latin hypercube sampling (LHS) [22] to generate the input data points which results in an even distribution of training points in the sample space. Further, the input domain spanning all three input variables considered in this study was chosen to capture the effects of needling and thinning on surface recession of the exposed char layer (Figure 1). The details of the input domain spanning all three dimensions are provided in Table 1 for reference.

Table 1: Ranges of the input parameter space used to develop the custom framework.

Porosity (ϕ)	Microscopic reaction probability (α)	Time (s)
0.79 - 0.94	0.002 - 0.04	Complete oxidation of the material

The predictive model is trained by the mesh files recorded from coupled flow-material simulations, performed at 100 random combinations of porosities and reaction probabilities in the specified domain. The 100 sampling cases resulted in a total of 100 × 20 mesh files (2000). The mesh files obtained from

the flow-material simulations [19] are processed to extract the surface function parameter. In-house Python scripts were developed to automate all the processes involved in data collection required for the SVR formulation. Further, the training data was scaled according to natural logarithmic values followed by SVR training to obtain the SVR formulation presented by Equation 4.

$$h(t, \phi, \alpha) = \exp\left(-8.73 + \sum_{i=1}^{488} (\boldsymbol{\alpha_i} - \boldsymbol{\alpha_i^*}) \exp(50\,\|\boldsymbol{x}_i - \boldsymbol{X}\|^2)\right) \tag{4}$$

Equation 4 is identical to the general form of SVR formulation (Equation. 3) presented in Sec. 2.2. The SVR formulation consists of 488 support vectors ($\boldsymbol{X}$) and their corresponding dual co-efficients ($\boldsymbol{\alpha_i} - \boldsymbol{\alpha_i^*}$), with -8.72 forming the intercept (b). Equation 4 can be used to obtain the height of an arbitrary char layer, which upon taking the partial derivative over t gives the recession rate. The hyper-parameters involved in the SVR formulation [21] were optimized on the training data and separate sets of test data to ensure the robustness of the developed supervised learning framework.

3.2 *Verification*

The main goal of the current study is to capture the changes in recession rate with variation in reaction probabilities. In order to prove the credibility of the developed model in capturing the recession rate, we present two test cases (Figure 5 and Figure 6) that undergo needling and thinning degradation respectively.

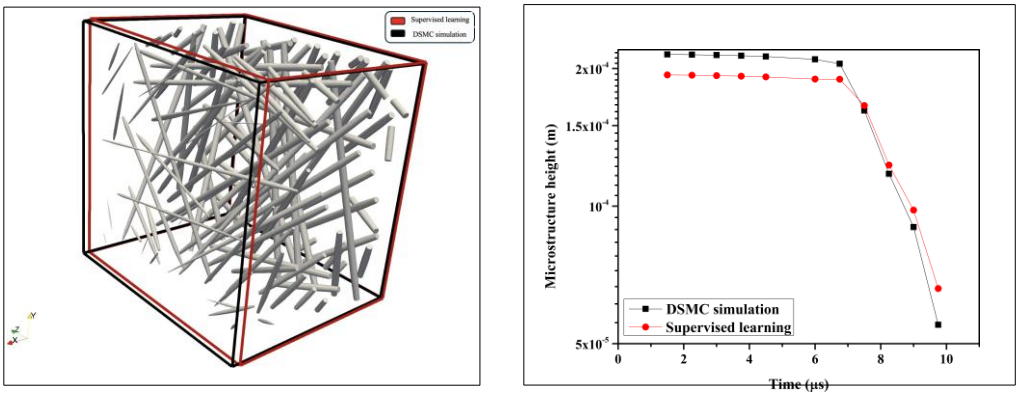

(a) (b)

Figure 5: Comparison of a predicted profile of a microstructure with actual profile at a microscopic reaction probability (α) of 0.028 (Figure 5(a)) and the comparison of the variation of microstructure height as the material degrades (Figure 5(b)).

Figure 5(a) represents the comparison of predicted degradation of a microstructure with actual profiles at an initial porosity of 0.84 and a reaction probability of 0.028. The predicted height of the microstructure (Figure 5(b)) can be utilized to find the associated recession rate as explained in Sec. 2.1. As discussed in Sec. 1 and presented in Figure 2(a), at high microscopic reaction probabilities, the microstructure experiences rapid consumption of material which results in a needle-like degradation of fibers which is evident from Figure 5(a). Rapid consumption of material at higher oxidation rates leads to a uniform recession rate, which is what we intended to capture through the predictive model. Figure 6(a) represents the comparison of the predicted degradation of a microstructure with actual profiles at an initial porosity of 0.88 and a reaction probability of 0.009. As discussed in Sec. 1 and presented in Figure 2(b), at low microscopic reaction probabilities, the microstructure experiences negligible changes until sufficient build up of oxygen atoms, which is then followed by spontaneous

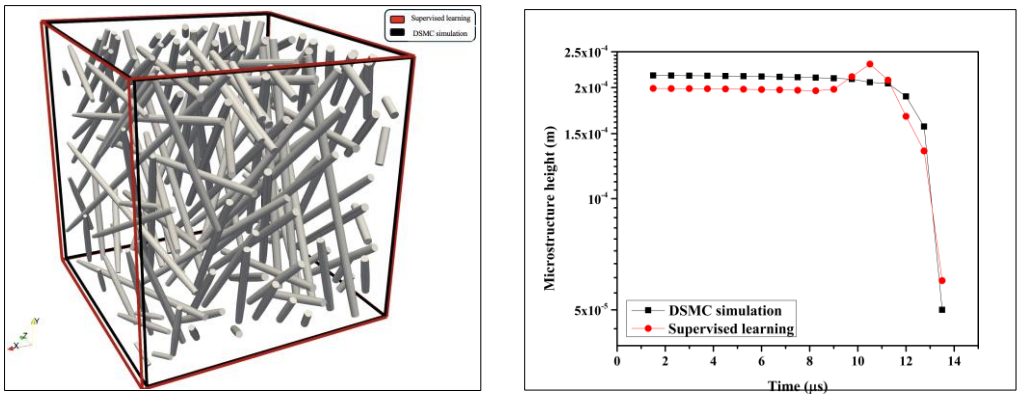

(a) (b)

Figure 6: Comparison of a predicted profile of a microstructure with actual profile at a microscopic reaction probability (α) of 0.009 (Figure 6(a)) and the comparison of the variation of microstructure height as the material degrades (Figure 6(b)).

consumption of the material (Figure 6(b)). This phenomenon results in a varying recession rate which is being captured by the developed model. Thus, we can conclude that the predictive model is able to distinguish between the thinning and needling types of oxidation along with their effects on surface recession for the above two test cases.

However, an extensive error analysis of test cases throughout the training domain should be considered before encouraging the idea of replacing the current model with mesoscale simulations. Further refinement of the current model may be necessary once we perform error analysis. The refinement would typically involve the optimization of the trained hyperparameters with in-house grid search algorithms or other sub-sampling techniques. Refinement of the current model lies outside the scope of the current study and will be performed in the future.

4 Conclusions and future work

In the current study, we developed a supervised learning model capable of determining the recession rate of an arbitrary microstructure exposed to hot dissociated oxygen atoms. The proposed framework helps in determining the recession rate of an arbitrary synthetic char layer with respect to a set of input variables. The trained model was capable of distinguishing between two distinct types of oxidation and had the capability to capture the corresponding recession rate. With the conceptualization and preliminary efforts of validation of the developed model, we were able to provide a proof of concept that successfully demonstrated the capabilities of machine learning techniques in providing a time and cost-effective alternative solution to the underlying spatio-temporal system.

In future iterations, we wish to develop separate models for predicting the recession rates of real C-C microstructures and char layers as opposed to synthetic microstructures. The developed framework needs to be re-done to include the influences of reactant and product species other than the ones considered in the present work. In the final iteration, we intend to develop a predictive model capable of capturing the physical changes of the entire microstructure as opposed to just the recession rate.

5 Acknowledgments

This work was supported by a Space Technology Research Institutes grant from NASA's Space Technology Research Grants Program under grant number 80NSSC21K1117. We would like to thank the University of Kentucky Center for Computational Sciences and Information Technology Services Research Computing for their support and use of the Morgan Compute Cluster and associated research

computing resources.

References

[1] M. M. Harussani et al. "Recent applications of carbon-based composites in defence industry: A review". In: *Defence Technology* 18 (8 2022). Issn: 22149147. doi: 10.1016/j.dt.2022.03.006.

[2] Akio Shindo. "Some Properties of PAN-based Carbon Fibre". In: *Journal of the Ceramic Society of Japan - Millennial Special* 69 (6 2000).

[3] Jean Lachaud et al. "Ablation workshop test case". In: *4th Ablation Workshop*. 2011.

[4] Savio Poovathingal and Thomas E. Schwartzentruber. "Effect of microstructure on carbon-based surface ablators using DSMC". In: *52nd Aerospace Sciences Meeting* (2014). doi: 10.2514/6.2014-1210.

[5] Ching Hsue Cheng and Huei Yuan Shiu. "A novel GA-SVR time series model based on selected indicators method for forecasting stock price". In: *Proceedings - 2014 International Conference on Information Science, Electronics and Electrical Engineering, ISEEE 2014* 1 (2014). doi: 10.1109/InfoSEEE.2014.6948139.

[6] Alexandre Martin and Iain Boyd. "CFD Implementation of a novel carbon-phenolic-in-air chemistry model for atmospheric re-entry". In: 2011. doi: 10.2514/6.2011-143.

[7] William H. Bowman and Richard M. Lawrence. "Space resources for teachers: Ablative materials for high-temperature thermal protection of space vehicles". In: *Journal of Chemical Education* 48 (10 1971). Issn: 00219584. doi: 10.1021/ed048p690.

[8] Savio Poovathingal et al. "Nonequilibrium flow through porous thermal protection materials, Part II: Oxidation and pyrolysis". In: *Journal of Computational Physics* 380 (2019), pp. 427–441.

[9] Eric C Stern et al. "Nonequilibrium flow through porous thermal protection materials, Part I: Numerical methods". In: *Journal of Computational Physics* 380 (2019), pp. 408–426. doi: https://doi.org/10.1016/j.jcp.2017.09.011.

[10] Krishna Sandeep Prata, Timothy K. Minton, and Thomas E. Schwartzentruber. "Air-Carbon Ablation Model for Hypersonic Flight from Molecular Beam Data". In: *AIAA Scitech 2021 Forum*. AIAA, 2021. doi: 10.2514/6.2021-0925. eprint: https://arc.aiaa.org/doi/pdf/10.2514/6.2021-0925. URL: https://arc.aiaa.org/doi/abs/10.2514/6.2021-0925.

[11] Sepp Hochreiter and Jürgen Schmidhuber. "Long Short-Term Memory". In: *Neural Computation* 9 (8 1997). Issn: 08997667. doi: 10.1162/neco.1997.9.8.1735.

[12] Pantelis R. Vlachas et al. "Data-driven forecasting of high-dimensional chaotic systems with long short-Term memory networks". In: *Proceedings of the Royal Society A: Mathematical, Physical and Engineering Sciences* 474 (2213 2018). Issn: 14712946. doi: 10.1098/rspa.2017.0844.

[13] Zheng Zhao et al. "LSTM network: A deep learning approach for Short-term traffic forecast". In: *IET Intelligent Transport Systems* 11 (2 2017). Issn: 1751956X. doi: 10.1049/iet-its.2016.0208.

[14] Mohamed Akram and Chaker El. "Sequence to Sequence Weather Forecasting with Long Short-Term Memory Recurrent Neural Networks". In: *International Journal of Computer Applications* 143 (11 2016). doi: 10.5120/ijca2016910497.

[15] David Montes de Oca Zapiain, James A. Stewart, and Rémi Dingreville. "Accelerating phase-field-based microstructure evolution predictions via surrogate models trained by machine learning methods". In: *npj Computational Materials* 7 (1 2021). Issn: 20573960. doi: 10.1038/s41524-020-00471-8.

[16] Alex Graves et al. "A novel connectionist system for unconstrained handwriting recognition". In: *IEEE Transactions on Pattern Analysis and Machine Intelligence* 31 (5 2009). Issn: 01628828. doi: 10.1109/TPAMI.2008.137.

[17] Steven L. Brunton et al. "Discovering governing equations from data by sparse identification of nonlinear dynamical systems". In: *Proceedings of the National Academy of Sciences of the United States of America* 113 (15 2016). Issn: 10916490. doi: 10.1073/pnas.1517384113.

[18] Vijay B. Mohan Ramu, Qiang (Shawn) Cheng, and Savio J. Poovathingal. "Development of a custom supervised learning network to model ablation of TPS materials." In: *AIAA AVIATION 2023 Forum*. doi: 10.2514/6.2023-3618. eprint: https://arc.aiaa.org/doi/pdf/10.2514/6.2023-3618. URL: https://arc.aiaa.org/doi/abs/10.2514/6.2023-3618.

[19] Vijay B. Mohan Ramu and Savio J. Poovathingal. "Development of a Custom Supervised Learning Network To Determine the Recession Rate of Ablative Thermal Protection Systems Materials". In: *AIAA AVIATION FORUM AND ASCEND 2024*. AIAA, 1995, p. 4031. doi: 10.2514/6.2024-4031. eprint: https://arc.aiaa.org/doi/pdf/10.2514/6.2024-4031. URL: https://arc.aiaa.org/doi/abs/10.2514/6.2024-4031.

[20] Vladimir N. Vapnik. *The Nature of Statistical Learning Theory*. Springer, 1995. doi: 10.1007/978-1-4757-2440-0.

[21] F. Pedregosa et al. "Scikit-learn: Machine Learning in Python". In: *Journal of Machine Learning Research* 12 (2011), pp. 2825–2830.

[22] M. D. McKay, R. J. Beckman, and W. J. Conover. "A Comparison of Three Methods for Selecting Values of Input Variables in the Analysis of Output from a Computer Code". In: *Technometrics* (1979). Issn: 00401706. doi: 10.2307/1268522.